Theor Chim Acta (1996) 94: 311–331

Theoretica Chimica Acta

Study on the behavior of energy convergence in ab initio crystal orbital calculations

Hiroyuki Teramae

NTT Basic Research Laboratories, 3-1 Wakamiya, Morinosato, Atsugi, Kanagawa 243-01, Japan

Received: November 21, 1994/Accepted: September 9, 1996

Summary. This article studies the dependence on the cutoff scheme of *ab initio* crystal orbital calculations with no long-range correction. We have thoroughly studied the Namur cutoff and cell-wise cutoff schemes through calculations of polyethylene and LiH chains. The Namur cutoff gives the fastest energy convergence with respect to the number of neighbors (N_0). The energy convergence behavior with respect to N_0 depends on the basis set. The Namur cutoff shows the fastest convergence with the STO-3G basis set, intermediate convergence with the MINI basis set, and the slowest convergence with the (7*s*4*p*/3*s*) basis set. The cell-wise cutoff shows exactly the reverse order of the Namur cutoff. The Namur cutoff destroys the translational symmetry. Both the Namur cutoff and cell-wise cutoff schemes introduce slight asymmetry on the two equivalent C–C bonds of polyethylene when calculating with a C_2H_4 unit cell. The asymmetry with the Namur cutoff can be made to disappear by increasing N_0 a little. The calculations on two different unit-cell structures of *trans*-polyacetylene show the effect of the cutoff scheme on the total energy. Only the symmetric cutoff energies are the same. Disagreement related to the Namur cutoff disappears at $N_0 = 20$, however, that related to the cell-wise and modified symmetric cutoff schemes remains at $N_0 \leqslant 20$. The optimized geometry and vibrational frequency are not as sensitive to the cutoff method except with the symmetric cutoff. A compilation of all results shows that the Namur cutoff is the superior cutoff scheme when calculating the insulator using the minimal basis set, especially the STO-3G basis set.

Key words: Energy convergence – Crystal orbital calculations – Cutoff scheme

1 Introduction

Recent progress in *ab initio* crystal orbital calculations is closely related to the development of one-dimensional organic semiconductors, which typically employ polyacetylene chains. Those polymers have attracted much attention due to their intriguing physical properties such as electric conductivity. Along with the development of experimental works, many theoretical works using the *ab initio* crystal orbital method have been published. Because polyacetylene is a very simple polymer, it is suitable for tests involving such large-scale calculations.

These works have clarified the problem with actual applications of crystal orbital calculations. The most significant one is the disagreement in *ab initio* results

among the works by Kertész et al. [1–3], Karpfen and Höller [4], Suhai [5], Dovesi [6], and Teramae et al. [7], works that employed the same STO-3G basis set. The same situation arose with the calculation of polyethylene chains. There was disgreement in the optimized geometry between the works by Karpfen, and Teramae et al. [8]. This disagreement is caused by a difference in the method cutting off truncations of the electron–electron, electron–nucleus, and nucleus–nucleus interactions.

In a previous paper [9], we proposed a modification to our calculations which greatly diminished the disagreement between our works and the others. The convergence of absolute energy values with respect to the number of neighboring cells included in the calculation (hereafter referred to as convergence), however, was found to be very slow. Even after summations of the nearest 50 neighboring cells, the total energy convergence is still remained within 10^{-3} a.u. for STO-3G level calculations.

On the other hand, Delhalle et al. [10] proposed the multipole expansion technique as an approximation for long-range interactions to overcome this slow convergence. The long-range correction is performed within the space where exact calculation of the electron–electron, electron–nucleus, and nucleus–nucleus interactions are neglected. Their test calculation on a metallic LiH chain showed very fast convergence. Summation of only the three nearest neighbors was necessary to ensure convergence within 10^{-5} a.u. The success of André et al. [11] demonstrated that polyethylene and LiH chain energy converges within 10^{-6} a.u. using the same method. Karpfen and Beyer [13] also showed that long-range correction was necessary with cell-wise cutoff to obtain well converged energy values for the polyethylene chain.

It has not been confirmed, however, that long-range correction is really necessary to obtain well converged energy. Furthermore, it has not been confirmed whether or not the converged energies with and without long-range correction are identical, except for the metallic LiH chain mentioned above. To answer these questions, we implemented the cell-wise and Namur cutoff schemes without long-range correction in our crystal orbital program system, in addition to the symmetric and the modified symmetric cutoff schemes which have been used in our previous works. The purposes of the present work are to study the convergence behavior of energy with respect to the number of neighbors as it relates to these two cutoff methods and to show how to obtain reasonable energy with respect to the number of neighbors without extra approximation (long-range correction).

Section 2 summarizes the methods used in the present work. In Sect. 3, our results are compared with those in previous reports. A polyethylene chain and LiH chain are used as model polymers. Section 4 shows the influence of the selected basis set on the energy convergence behavior with respect to the number of neighbors. That section also shows how the accuracy of the two-electron integrals affects the total energy. In Sect. 5, the symmetry breaking problem is discussed. Section 6 shows the effect of differences in the unit-cell structure. Section 7 shows the convergence behavior of the optimized structure and the vibrational frequencies of the polymer with respect to the number of neighbors. Section 8 compares the CPU time required for the Namur and the cell-wise cutoff schemes. Conclusions based on the results obtained in this study are given in Sect. 9.

2 Methods of calculation

The *ab initio* crystal orbital theory is an extension of the molecular orbital theory for infinite systems [14, 15]. In this section, the crystal orbital theory and cutoff methods are summarized.

2.1 *Crystal orbital theory*

In the crystal orbital theory, the total wave function of the polymer is approximated by a single Slater determinant built with the one-electron wave function (crystal orbital), $\psi_n(\boldsymbol{r}, \boldsymbol{k})$. Each crystal orbital is further expanded by linear combination with the Bloch basis functions, $\phi_s(\boldsymbol{r}, \boldsymbol{k})$ such that

$$\psi_n(\boldsymbol{r}, \boldsymbol{k}) = \sum_{s=1}^{\text{basis}} C_{sn}\psi_n(\boldsymbol{k})\,\phi_s(\boldsymbol{r}, \boldsymbol{k}). \tag{1}$$

Here, $\boldsymbol{r}$ is the coordinate of the electron and $\boldsymbol{k}$ is the wave vector, basis denotes the number of basis functions, and is equivalent to the number of atomic basis functions in the unit cell.

The Bloch basis functions are represented by the Bloch sum of the atomic orbitals in the unit cell:

$$\phi_s(\boldsymbol{r}, \boldsymbol{k}) = 1/\sqrt{2N+1} \sum_{j=-N}^{+N} \exp(\mathrm{i}\boldsymbol{k}\boldsymbol{a}j)\,\chi_s(\boldsymbol{r} - j\boldsymbol{a}), \tag{2}$$

where $N = \infty$, $1/\sqrt{2N+1}$ is the normalization constant, and i is the imaginary number unit. $\chi_s(\boldsymbol{r} - j\boldsymbol{a})$ represents the sth atomic basis functions in the jth cell from the central unit cell. The usual Gaussian-type basis functions such as the STO-3G or 6-31G basis sets are used for these atomic basis functions.

The expectation value of the electronic energy per unit cell is expressed as

$$\frac{E_{\text{elec}}}{2N+1} = \frac{\boldsymbol{a}}{2\pi} \int_{-\pi/a}^{\pi/a} \sum_{n}^{\text{occupied}} C_n^*(\boldsymbol{k}) \times \{\boldsymbol{H}(\boldsymbol{k}) + \boldsymbol{F}(\boldsymbol{k})\}\, C_n(\boldsymbol{k})\, \mathrm{d}\boldsymbol{k}. \tag{3}$$

The definition of $\boldsymbol{H}$ and $\boldsymbol{F}$ are given in Eqs. (6) and (7). Integration is performed within the first Brillouin zone, $(-\pi/a < \boldsymbol{k} \leqslant \pi/a)$. Applying the ortho-normality condition,

$$\int \psi_n^*(\boldsymbol{r}, \boldsymbol{k})\psi_m(\boldsymbol{r}, \boldsymbol{k})\, \mathrm{d}\boldsymbol{r} = \delta_{nm} \tag{4}$$

for E_{elec}, and performing Ritz's variational method, the secular equations, i.e., the Fock equations, are derived as follows:

$$\varepsilon(\boldsymbol{k})\boldsymbol{S}(\boldsymbol{k})\boldsymbol{C}(\boldsymbol{k}) = \boldsymbol{F}(\boldsymbol{k})\boldsymbol{C}(\boldsymbol{k}). \tag{5}$$

$F_{rs}(\boldsymbol{k})$, $H_{rs}(\boldsymbol{k})$, and $S_{rs}(\boldsymbol{k})$ are represented by Fourier transforms of the matrix elements of real space which do not contain $\boldsymbol{k}$.

$$F_{rs}(\boldsymbol{k}) = \sum_{j=-N}^{+N} \exp(\mathrm{i}\boldsymbol{k}\boldsymbol{a}j)\,F_{rs}^{0j}, \tag{6}$$

$$H_{rs}(\boldsymbol{k}) = \sum_{j=-N}^{+N} \exp(\mathrm{i}\boldsymbol{k}\boldsymbol{a}j)\,H_{rs}^{0j}, \tag{7}$$

$$S_{rs}(\boldsymbol{k}) = \sum_{j=-N}^{+N} \exp(\mathrm{i}\boldsymbol{k}\boldsymbol{a}j)\,S_{rs}^{0j}. \tag{8}$$

If we define the sth atomic orbital in the jth unit cell from the central cell as $x_s(\boldsymbol{r}-j\boldsymbol{a}) \equiv \chi_s^j$, the matrix element of the overlap integrals is

$$S_{rs}^{0j} = \int \chi_r^0 \chi_s^j \, \mathrm{d}\boldsymbol{r} \equiv \langle \chi_r^0 | \chi_s^j \rangle. \tag{9}$$

The matrix element of the core Hamiltonian integrals is

$$H_{rs}^{0j} = -\frac{1}{2}\langle \chi_r^0 | \Delta | \chi_s^j \rangle - \sum_{h=-N}^{+N} \sum_{A}^{\text{atom}} \left\langle \chi_r^0 \left| \frac{Z_A}{|\boldsymbol{r} - \boldsymbol{R}_A^h|} \right| \chi_s^j \right\rangle, \tag{10}$$

where $\boldsymbol{R}_A^h$ represents the Ath atomic coordinate at the hth unit cell.

Finally, Fock matrix element is

$$F_{rs}^{0j} = H_{rs}^{0j} + \sum_{h=-N}^{+N} \sum_{l=-N}^{+N} \sum_{t}^{\text{basis}} \sum_{u}^{\text{basis}} P_{tu}^{hl} \times \{2\langle \chi_r^0 \chi_s^j | \chi_t^h \chi_u^l \rangle - \langle \chi_r^0 \chi_t^h | \chi_s^j \chi_u^l \rangle\}, \tag{11}$$

where the two-electron integral is

$$\langle \chi_r^0 \chi_s^j | \chi_t^h \chi_u^l \rangle = \int\int \chi_r^0(\boldsymbol{r}_1)^* \chi_s^j(\boldsymbol{r}_1) \times \frac{1}{r_{12}} \chi_t^h(\boldsymbol{r}_2) \chi_u^l(\boldsymbol{r}_2)^* \, \mathrm{d}\boldsymbol{r}_1 \, \mathrm{d}\boldsymbol{r}_2. \tag{12}$$

All integrals given above are easily obtained using the integral package in existing molecular orbital programs, such as the Gaussian or Hondo series. Note that the Fock matrix elements are calculated directly in our crystal orbital program. The two-electron integrals are not saved in disk storage but calculated repeatedly in each SCF step. This is done because the number of two-electron integrals easily exceeds 2 gigabytes, which is the largest file size of a 32-bit operating system.

The total density matrix elements P_{tu}^{hl}, appearing in the Fock matrix elements, are defined as

$$P_{tu}^{hl} = \frac{a}{\pi} \int_{-\pi/a}^{\pi/a} \sum_{n}^{\text{occupied}} \exp\{\mathrm{i}\boldsymbol{k}a(h-l)\} \times C_{tn}^*(\boldsymbol{k}) C_{un}(\boldsymbol{k}) \, \mathrm{d}\boldsymbol{k}. \tag{13}$$

Integration is performed within the first Brillouin zone ($-\pi/a < \boldsymbol{k} \leqslant \pi/a$).

From these relations, we can write the total energy in the real space independent of the wave vector $\boldsymbol{k}$:

$$\frac{E_{\text{total}}}{2N+1} = -\frac{1}{2} \sum_{j=-N}^{+N} \sum_{r}^{\text{basis}} \sum_{s}^{\text{basis}} (H_{rs}^{0j} + F_{rs}^{0j}) P_{rs}^{0j} + \frac{1}{2} \sum_{j=-N}^{+N} \sum_{A}^{\text{atom}} \sum_{B}^{\text{atom}} \frac{Z_A Z_B}{|\boldsymbol{R}_A^0 - \boldsymbol{R}_B^j|}, \tag{14}$$

where $A \neq B$ when $j = 0$. Z_A is the charge of the atomic nucleus A. The second term of the right-hand side is the nuclear repulsion energy, and the first term is the electronic energy equivalent to E_{elec}.

2.2 *Nth neighbor approximation*

Since the equations in the previous sections contain summation to infinity, we can not calculate them. For the first approximation, we terminate the calculations when the value of the integrals becomes sufficiently small. The nucleus–electron, electron–electron, and nucleus–nucleus interactions are electrostatic, and the decay is the order of r^{-1}. This means that if we set 10^{-8} Hartree as the threshold value, we can calculate all the integrals within the area of 10^8 Bohr. This is also impossible in practical applications. In addition, it should be noted that some studies previously pointed out that the convergence of the exchange terms may also be very slow [16], however, we will not treat the exchange problem in the present paper.

For the second approximation, we select a proper neighboring cell number N and consider only the basis functions within the Nth cell from the central one. All other basis functions are neglected. This is called *Nth neighbor approximation.* It is important in this approximation to select the cutoff method which further restricts the matrix elements within N neighbors.

2.2.1 *No cutoff*

No cutoff scheme is simple and straightforward. All summation from $-N_0$ to N_0 are considered, where N_0 is a finite number such that summations up to infinity are approximated as

$$\sum_{j=-N}^{+N}\sum_{h=-N}^{+N}\sum_{l=-N}^{+N} \rightarrow \sum_{j=-N_0}^{+N_0}\sum_{h=-N_0}^{+N_0}\sum_{l=-N_0}^{+N_0}. \tag{15}$$

This was used in earlier *ab initio* calculations [17], but is not used now. It is now used only in semi-empirical calculations such as the CNDO/2 method [18, 19]. Because there are no three- or four-center integrals, there is no choice about the cutoff scheme in the CNDO/2 method. The total energy convergence with respect to N_0 is very slow and some symmetric properties are destroyed. For example, the Coulomb integral, $\langle \chi_r^0 \chi_s^0 | \chi_t^{-N} \chi_u^N \rangle$ is not neglected but the corresponding density matrix element, $P_{t\ u}^{-N\ N} = P_{t\ u}^{0\ 2N}$, is. We did not use this cutoff method in this study.

2.2.2 *Cell-wise cutoff*

This summation is performed in the following steps. Summation over j:

$$\sum_{j=-N}^{+N} \rightarrow \sum_{j=-N_0}^{N_0} \tag{16}$$

is the same as having no cutoff, however, summations over h and l are restricted such that [20]

$$\sum_{h=-N}^{+N}\sum_{l=-N}^{+N} \rightarrow \begin{cases} \displaystyle\sum_{h=-N_0+j}^{N_0}\sum_{l=-N_0+j}^{N_0} & (j \geqslant 0), \\ \displaystyle\sum_{h=-N_0}^{N_0+j}\sum_{l=-N_0}^{N_0+j} & (j < 0). \end{cases} \tag{17}$$

The difference between the cell indices appearing in the nucleus–electron and electron–electron interactions (core-attraction integrals and two-electron integrals) arises within $\pm N_0$. Thus, the h and l values depend on the j value and are symmetric with respect to both the central cell and the jth cell.

2.2.3 Namur-type cutoff

The Namur group proposed this cutoff with long-range correction by the multipole expansion technique [11]. The Namur-type cutoff takes the summation for a set of cell indices $(0, j)$ and (h, l) to be symmetric, i.e.

$$\sum_{j=-N}^{+N}\sum_{h=-N}^{+N}\sum_{l=-N}^{+N} \rightarrow \sum_{j=-N_0}^{N_0}\sum_{h=-N_0'}^{N_0'}\sum_{l=-N_0+h}^{N_0+h}. \tag{18}$$

It is characteristic that the summation of l exceeds N_0. In this article, we set N_0' equal to N_0 except in the case of the direct comparison of our results with the work of André et al. [11].

The defect of this cutoff is a breaking of the translational invariance of the Fock matrix elements. This is very serious because the Fock matrix does not become an Hermitian matrix. We, therefore, cannot solve the Fock equations in Eq. (5). In this article, we simply impose a symmetry on Fock matrix elements,

$$F_{sr}^{0-j} = F_{rs}^{0j} \quad (\text{for } j \geqslant 0) \tag{19}$$

as an extra approximation in constructing the $\boldsymbol{k}$-dependent Fock matrix element in Eq. (6).

2.2.4 Symmetric cutoff

The above cutoff methods do not completely satisfy the symmetry condition if there are symmetrically equivalent bonds in the inter- and intra-cell bonds. For example, when calculating the crystal orbitals of *trans*-polyethylene with a C_2H_4 unit cell, the inter- and intra-cell C–C bonds are equivalent. The cutoff methods mentioned in the previous subsections cannot describe in principle the fact that these two bonds are equivalent.

The symmetric cutoff method uses the cutoff radius $\boldsymbol{r}_{\text{cutoff}}$ instead of the cell number N_0 to avoid the symmetry problem. The matrix element between the basis functions separated by more than the length of $\boldsymbol{r}_{\text{cutoff}}$ is discarded. There is, however, ambiguity as to how to select the cutoff radius. We have proposed the modified symmetric cutoff scheme [9] to overcome this ambiguity. In the original symmetric cutoff scheme uses the cutoff radius

$$\boldsymbol{R}_{\text{cutoff}} = n\boldsymbol{a}, \tag{20}$$

whereas the modified symmetric cutoff uses the cutoff radius

$$\boldsymbol{R}_{\text{cutoff}} = \min(\boldsymbol{R}_{AB}^{0,n+1}), \tag{21}$$

where $\boldsymbol{R}_{AB}^{0,n+1}$ denotes the atomic distance between the Ath atom in the central cell and the Bth atom in the $(n+1)$th cell.

Suhai proposed to use different cutoff radii for the different integrals [12]. He claimed that the single cutoff radius should not be used to keep the translation symmetry and electrical neutrality, however, in the present paper, we attempt to use the single cutoff radius only because his calculations on the polyacetylene chain showed quite good agreement with our previous calculations.

2.3 Use of helical symmetry

In the following section, we used a combined symmetry operation rather than a simple translation to calculate the crystal orbitals of the polyethylene chain. If we

take the screw axis coincident with the Cartesian z-axis, the $\tilde{p}_x^j$ and $\tilde{p}_y^j$ basis functions belonging to the jth cell from the reference cell can be obtained by rotating the Cartesian p_x^j and p_y^j orbitals. By performing these rotations on all one- and two-electron integrals, we are able to take one CH_2 unit itself as the unit cell where the helical angle is 180°. This idea was first implemented by Imamura for extended Hückel calculations [21]. It was then applied to the CNDO/2 version by Fujita and Imamura [22] and Morokuma [23, 24], in succession. The *ab initio* level calculations were finally reported by Blumen and Merkel [25]. Very recently, this procedure has been applied to more realistic polymer systems [11, 13, 26, 27].

2.4 Wave vector sampling

The density matrix elements, Eq. (13), contain the integral with respect to the wave vector $\boldsymbol{k}$. This integration must be performed using an appropriate numerical integration rule. In this paper, we use Simpson's rule [28] and the number of sampling points (half the Brillouin zone) is 21 points for $N_0 = 2 - 10$, 41 points for $N_0 = 11$–20, 101 points for $N_0 = 21$–50, 201 points for $N_0 = 51$–100, and 401 points for $N_0 = 149$. These values can arbitrarily be chosen, as long as they are not smaller than N_0. Smaller values, however, inevitably cause numerical errors.

3 Cutoff dependence on total energy convergence

The energy convergence behavior of the polyethylene chain with the STO-3G basis set is shown in Table 1. The geometry used here is the one optimized by Karpfen [29]; $r_{CC} = 1.547$ Å, $r_{CH} = 1.089$ Å, $\angle$ HCH = 107.0°, and $\angle$ CCC = 112.6°. Results for the Namur and cell-wise cutoffs are shown in the table. The results for symmetric cutoff are identical with those for cell-wise cutoff in this case. Our results for cell-wise cutoff are almost identical with those of Karpfen and Beyer [13],

Table 1. Energy convergence behavior of polyethylene with the STO-3G basis set. N_0 represents the number of neighboring CH_2 units. Energy units are shown in a.u.

N_0	Namur[a]	Cell-wise[a]	Cell-wise[b]	Cell-wise LC[b, c]
2	−38.576910	−38.580047	—	—
3	−38.580221	−38.581911	—	—
4	−38.580196	−38.581206	—	—
5	−38.580196	−38.580872	−38.58087	−38.58023
6	−38.580196	−38.580678	−38.58067	−38.58019
7	−38.580196	−38.580558	−38.58055	−38.58019
8	−38.580196	−38.580477	—	—
9	−38.580196	−38.580421	—	—
10	−38.580196	−38.580380	—	—
20	−38.580196	−38.580244	—	—
50	−38.580196	−38.580204	—	—
100	−38.580196	−38.580198	—	—

[a] Present work

[b] From the work of Karpfen and Beyer [13]

[c] Cell-wise with long-range correction

Table 2. Energy convergence behavior of helical polyethylene with the STO-3G basis set. The helical angle is 80 degrees. N_0 represents the number of neighboring CH_2 units. Energy units are shown in a.u.

N_0	Namur[a]	Cell-wise with LC[b]
2	−38.585129	—
3	−38.579270	—
4	−38.570715	—
5	−38.572139	—
6	−38.572116	—
8	−38.572111	−38.52115
10	−38.572111	−38.57208
12	−38.572110	−38.57213
14	−38.572109	−38.57213
20	−38.572109	—

[a] Present work

[b] Cell-wise with long-range correction, from the work of Karpfen and Beyer [13]

which are also shown in Table 1 for comparison. The total energy convergence is remarkably fast at the Namur cutoff level. The energy converges at $N_0 = 4$ within an accuracy of 10^{-6} a.u. It should be noted that the Namur energy converges faster than the cell-wise energy after long-range correction.

To confirm the above, we also calculated the energy convergence in polyethylene with a helical angle of 80°, as shown in Table 2. Karpfen and Beyer [13] reported that the convergence was very slow in this configuration and that the multipole expansion approximation for long-range terms deteriorated below a critical number of neighbors ($N_0 = 8$ in this case). The present Namur energy converges within 10^{-5} a.u. at $N_0 = 8$ and 10^{-6} a.u. at $N_0 = 14$. The error is only 3×10^{-5} a.u. even at $N_0 = 5$. Note that the energy values for $N_0 = 2$–4 are unreliable, because one helical turn is not yet completed.

Tables 3 and 4 compare the present results with those of André et al. [11] which include long-range correction by multipole expansion. The minimal contraction of Clementi's (7*s*3*p*/4*s*) basis set [30] (hereafter referred as (7*s*3*p*/4*s*) basis set) is used to calculate the convergence in the polyethylene chain, and the STO-3G basis set [31] is used for the linear LiH chain. The geometry is taken from the work of André et al. [32]; $r_{CC} = 1.54$ Å, $r_{CH} = 1.09$ Å, $\angle$ CCC = 109.5°, and $\angle$ HCH = 109.5° for the polyethylene; $r_{LiH} = 4$ a.u. and $r_{HLi} = 6$ a.u. for the LiH chain.

It is interesting to note that our polyethylene energy converges a little faster than that of André et al. Long-range correction seems to disturb the energy convergence in this case. On the other hand, the LiH energy with long-range correction converges faster. The slight difference in the converged energy is thought to be due to numerical errors. Because the LiH chain is more ionic than the polyethylene chain, multipole approximation works well in this case.

4 Basis set dependence of total energy convergence

In comparing Tables 1 and 3, we noticed that the energy convergence behavior depends on the basis set. The STO-3G energy converges at $N_0 = 4$ but the (7*s*3*p*/4*s*)

Table 3. Energy convergence behavior of polyethylene with Clementi's (7*s*3*p*/4*s*)/[2*s*1*p*/1*s*] basis set. Energy units are shown in a.u.

N_0	N_0'	Namur[a]	Namur with LC[b]
5	9	−38.879792	−38.866876
9	17	−38.879775	−38.879876
11	21	−38.879775	−38.879806
11	37	−38.879774	−38.879786
11	49	−38.879774	−38.879784
13	49	−38.879774	−38.879775
17	49	−38.879774	−38.879773
19	37	−38.879774	−38.879775
19	49	−38.879774	−38.879773

[a] Present work
[b] From the work of André et al.: The Namur cutoff with long-range correction by the multipole expansion technique [11]

Table 4. Energy convergence behavior of an LiH chain with the STO-3G basis set. Energy units are shown in a.u.

N_0	N_0'	Namur[a]	Namur with LC[b]
3	5	−7.841428	−7.841404
5	9	−7.841446	−7.841445
7	13	−7.841451	−7.841448
9	17	−7.841453	−7.841449
9	25	−7.841455	−7.841449
9	49	−7.841456	−7.841449
9	99	−7.841456	−7.841449

[a] Present work
[b] From the work of André et al.: The Namur cutoff with long-range correction by the multipole expansion technique [11]

energy does not, even at $N_0 = 11$ ($N_0' = 21$). We continued by calculating polyethylene chains with the (7*s*3*p*/4*s*) basis set and Huzinaga's MINI-1 basis set. The results are shown in Table 5. The geometry is the same as that adopted in the previous section for the (7*s*3*p*/4*s*) basis set.

It is clear from Table 5 that the convergence of cell-wise cutoff is greatly improved with these two basis sets. The Namur energy converges slower than that of STO-3G. As a result, the difference between the Namur and cell-wise cutoffs becomes negligible, although the Namur energy converges a little bit faster. Both converge at $N_0 = 9$ within 10^{-5} a.u. Table 5 shows that the MINI-1 basis set gives the intermediate behavior between the STO-3G and (7*s*3*p*/4*s*) results. 10^{-5} a.u. accuracy is achieved at $N_0 = 6$ for the Namur cutoff and $N_0 = 9$ for cell-wise cutoff.

The energy convergence dependence on the basis set is related to the diffusivity of the spatial distribution of the basis set. The most diffused basis set (7*s*3*p*/4*s*) is relatively insensitive to the cutoff method, however, sufficient convergence is never obtained for the most compact basis set STO-3G without the Namur cutoff. Thus, use of the STO-3G basis set is not recommended in crystal orbital calculations.

Indeed, the serious disagreements among the past computational results for the polyacetyene, polyethylene, and other polymers, are now attributed to the use of the STO-3G basis set.

On the other hand, the extended basis sets, such as double-zeta and split-valence basis sets, generally have more diffused orbital exponents than the STO-3G basis set and are expected to show faster convergence. In our previous work on polyacetylene with the modified symmetric cutoff scheme, the 4-31G results indeed showed sufficiently faster convergence than that seen in the STO-3G results [9]. Table 6 shows the 3-21G and 4-31G results of the polyethylene calculations in

Table 5. Energy convergence behavior of polyethylene with Clementi's 7*s*3*p*/4*s* basis set and the MINI-1 basis set. Energy units are shown in a.u.

	7*s*3*p*/4*s*		MINI-1	
N_0	Namur	Cell-wise	Namur	Cell-wise
2	−38.862465	−38.860464	−38.736853	−38.735063
3	−38.880480	−38.880456	−38.752940	−38.752873
4	−38.879844	−38.879825	−38.752455	−38.752420
5	−38.879818	−38.879826	−38.752437	−38.752439
6	−38.879785	−38.879787	−38.752426	−38.752428
7	−38.879788	−38.879792	−38.752425	−38.752431
8	−38.819077	−38.819092	−38.752421	−38.752426
9	−38.879780	−38.879782	−38.752422	−38.752427
10	−38.879774	−38.879776	−38.752420	−38.752425
20	−38.879774	−38.879774	−38.752420	−38.752422
50	−38.879774	−38.879774	−38.752420	−38.752420
100	−38.879775	−38.879775	−38.752420	−38.752420

Table 6. Energy convergence behavior of polyethylene with the 3-21G and 4-31G basis sets. NC means the SCF step was not converged. Energy units are shown in a.u.

	3-21G		4-31G	
N_0	Namur	Cell-wise	Namur	Cell-wise
2–4	NC	NC	NC	NC
5	−38.819140	−38.819254	NC	NC
6	−38.819113	−38.819122	NC	NC
7	−38.819080	−38.819122	−38.977576	−38.977579
8	−38.819077	−38.819092	−38.977578	−38.977562
9	−38.819073	−38.819094	−38.977570	−38.977572
10	−38.819071	−38.819081	−38.977570	−38.977565
15	−38.819070	−38.819075	−38.977568	−38.977569
20	−38.819068	−38.819071	−38.977567	−38.977567
50	−38.819068	−38.819069	−38.977567	−38.977568
100	−38.819069	−38.819069	−38.977568	−38.977568

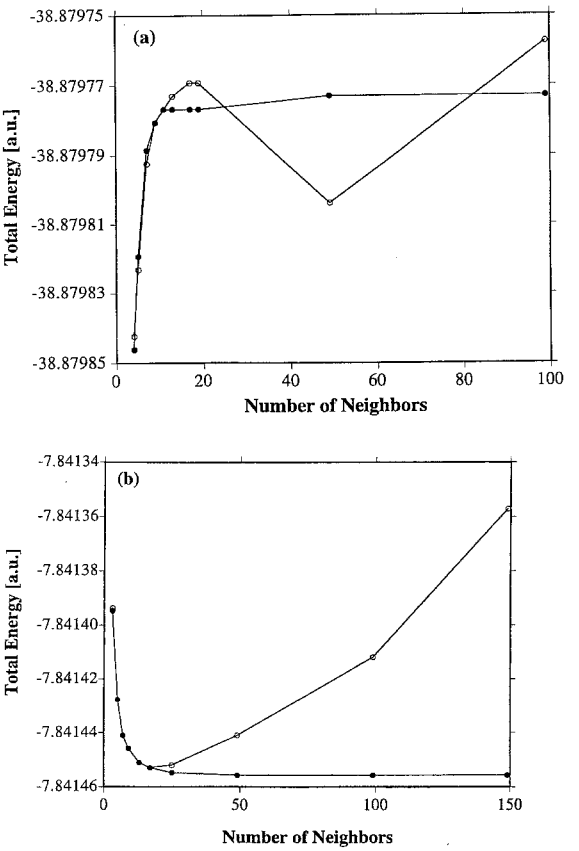

Fig. 1. Effect of the two-electron integral threshold values on the total energy convergence of (a) polyethylene with the (7*s*3*p*/4*s*) basis set and (b) an LiH chain with the STO-3G basis set. Open and closed circles correspond to the 10^{-6} and 10^{-8} threshold values of the two-electron integrals

Karpfen's geometry [29]. The cell-wise cutoff results show sufficient convergence for both basis set levels.

We would also like to mention the cutoff threshold of the two-electron integrals. Cutoff means the two-electron integrals below the threshold value are discarded in constructing the Fock matrix. In all our previous work, we employed 10^{-6} as the threshold value. We have now found that this threshold value was insufficient when including a large number of neighboring interactions. Figure 1 shows the dependence of the total energy on the threshold value of the two-electron integrals. Both cases use the Namur cutoff and in both cases, the 10^{-8} threshold value is needed to ensure stable convergence. The energy values obtained in the calculation with the 10^{-6} threshold value seem to be incorrect in the regions including a large number of neighbors. For polyethylene, these are the regions in which $N_0 > 10$ and for the LiH chain, $N_0 > 20$.

We feel, therefore, the necessity to reconsider of our previous work [9] in which we calculated convergence in polyacetylene chains with a 10^{-6} threshold value. Table 7 compares the STO-3G total energies of *trans*-polyacetylene with those given in our previous work. It is clear that inappropriate selection of the threshold value can cause slow convergence.

Table 7. Total energy of all-*trans*-polyacetyene with the STO-3G basis set corresponding to the threshold values for the two-electron integrals 10^{-8} and 10^{-6}. Energy units are shown in a.u.

N_0	10^{-8} [a]	10^{-6} [b]
4	−75.954235	−75.95423
6	−75.952046	−75.95204
8	−75.950974	−75.95096
10	−75.948108	−75.94810
14	−75.948025	−75.94801
18	−75.947989	−75.94796
22	−75.947971	−75.94792
26	−75.947961	−75.94789
30	−75.947954	−75.94786
40	−75.947946	−75.94775
50	−75.947941	−75.94762

[a] Present work
[b] From Ref. [9]

5 Symmetry breaking problem

The Namur cutoff always breaks symmetry and the cell-wise cutoff does not always retain symmetry. This symmetry breaking problem typically appears when calculating crystal orbitals in polyethylene with a double-size unit cell, that is $(C_2H_4)_x$.

Table 8 shows the crystal orbital coefficients of polyethylene at the top of the valence band. Although the coefficients for two carbon atoms should be the same, the Namur results exhibit slight asymmetry. This asymmetry, however, is considered to be too small to affect the results. The cell-wise results also shown in Table 8 indicate maintained symmetry.

Table 9 shows the density matrix elements between the $2p_z$ orbitals (Fig. 2). These inter- and intra-cell elements should be the same. The degree of asymmetry is highest with cell-wise cutoff, as reported earlier [33], and does not disappear within the tenth-neighbor approximation. The Namur cutoff also exhibits asymmetry at $N_0 = 2$, however, it is relatively slight and disappears within five decimal points when the number of neighbors is extended beyond 3. The modified symmetric cutoff, of course, does not break symmetry.

One more important effect of the asymmetry is seen in the total energy. Table 10 shows the total energy of polyethylene with the STO-3G basis set and a double-size unit cell. It is clear that the total energy results for the cell-wise cutoff do not agree with those for a single-size unit cell given in Table 1. The N_0 neighbors results in Table 10 should agree with the $2N_0$-neighbors results in Table 1. Note, however, that agreement arises between the cell-wise results in Table 1 and the modified symmetric cutoff results in Table 10. Because the results of the modified symmetric and cell-wise cutoff for the CH_2 unit cell is the same, this symmetry condition is preserved in the modified symmetric cutoff scheme. The Namur cutoff is not expected to satisfy the symmetry condition in principle, however, the total energy converges even at $N_0 = 4$ (Table 1). Thus, effect of this asymmetry is considered to be negligible when calculating the insulator. We would like to note,

Table 8. Crystal orbital coefficients at the top of the valence band of polyethylene with the Namur cutoff

N_0		2	3	4	5	10	2[a]
C	1s	−0.00023	0.00004	−0.00001	0.00000	−0.00000	0.00144
	2s	0.00090	−0.00016	0.00003	−0.00001	0.00001	−0.00567
	2px	0.00000	−0.00000	−0.00000	−0.00000	0.00000	0.00000
	2py	−0.00167	0.00032	−0.00006	0.00001	−0.00002	0.01244
	2pz	−0.65810	0.65811	−0.65810	0.65811	−0.65810	−0.65790
H	1s	−0.00095	0.00018	−0.00003	0.00001	−0.00001	0.00650
H	1s	−0.00095	0.00018	−0.00003	0.00001	−0.00001	0.00650
C	1s	−0.00023	0.00004	−0.00001	0.00000	−0.00000	0.00144
	2s	0.00090	−0.00017	0.00003	−0.00001	0.00001	−0.00567
	2px	0.00000	0.00000	0.00000	0.00000	0.00000	0.00000
	2py	0.00165	−0.00031	0.00005	−0.00001	0.00002	−0.01244
	2pz	0.65809	−0.65810	0.65810	−0.65809	0.65810	0.65790
H	1s	−0.00095	0.00018	−0.00003	0.00001	−0.00001	0.00650
H	1s	−0.00095	0.00018	−0.00003	0.00001	−0.00001	0.00650

[a] Cell-wise cutoff

Table 9. Density matrix elements between the nearest carbon $2p_z$ orbitals

N_0	Namur		Cell-wise		MSC[a]	
	C_1^0–C_2^0	C_2^0–C_1^1	C_1^0–C_2^0	C_2^0–C_1^1	C_1^0–C_2^0	C_2^0–C_1^1
2	−0.36024	−0.36026	−0.36259	−0.35876	−0.36077	−0.36077
3	−0.36025	−0.36025	−0.36134	−0.35957	−0.36049	−0.36049
4	−0.36025	−0.36025	−0.36088	−0.35987	−0.36039	−0.36039
5	−0.36026	−0.36026	−0.36066	−0.36011	−0.36034	−0.36034
10	−0.36034	−0.36034	−0.36043	−0.36026	−0.36034	−0.36034

[a] Modified symmetric cutoff

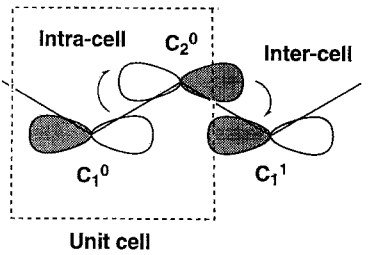

Fig. 2. The $2p_z$ orbitals defined in Table 9, inter and intra denote inter- and intra-cell interactions

however, that in some cases the slight asymmetry introduced by Namur and cell-wise cutoff methods are not acceptable, because the symmetry is exact. For example, these cutoff methods cannot correctly describe the potential energy surface of the polyacetylene chain around $r_1 - r_2 = 0$, where r_1 and r_2 denote the bond lengths of the single and double bonds, respectively, [34]. Only the symmetric cutoff method will give correct results in such a case.

Table 10. Total energy of polyethylene with a double-size unit cell. Energy is given in a.u.

N_0	Namur	Cell-wise	MSC[a]
2	−77.160392	−77.162093	−77.162412
3	−77.160393	−77.161239	−77.161356
4	−77.160393	−77.160899	−77.160954
5	−77.160393	−77.160730	−77.160760
10	−77.160393	−77.160484	−77.160488

[a] Modified symmetric cutoff

6 Dependence on unit-cell structure

There is some ambiguity involved in the selection of the unit-cell structure. Figure 3 shows the two types of unit cells of all-*trans*-polyacetylene with exactly the same crystal structure. All previous works employed only Type 1. Computational results obtained by the crystal orbital method usually depend on the unit-cell structure because the Fock matrix element is first evaluated in real space, as described in Section 2. This is a specific problem in Hartree–Fock crystal orbital calculations. In other energy band computational methods using the local-density functional approach, summation is usually performed directly in $\boldsymbol{k}$-space, and there is no problem.

Table 11 shows the total energy of polyacetylene with the STO-3G basis set using the two different unit cells. The symmetric cutoff, by definition has no dependence, although the total energy convergence is much slower than with the other cutoff schemes, all of which exhibit some dependence. The Namur cutoff results in the smallest difference, which rapidly decreases with increasing N_0. After summation of 20 neighbors ($N_0 = 20$), the results are identical, within 10^{-6} a.u. Results for the other two schemes, cell-wise and modified symmetric, never become identical in our calculations ($N_0 \leqslant 20$). Note that the results for the cell-wise and modified symmetric cutoff in the Type 1 structure are the same at $N_0 = 10$ and 20.

A more significant problem is the difference in the energy band structure. Figure 4 shows the energy band structures at $N_0 = 3$ with Namur and cell-wise cutoff. In the Namur scheme, the results for Types 1 and 2 unit-cells are almost the same. In the cell-wise scheme, however, the results are significantly different. This is attributed to the slow convergence of the oribital eigenvalues in the cell-wise cut off scheme, as mentioned in Sect. 6. Fortunately, this difference seems to be only a parallel movement of the absolute value, so the shape of the energy band structure does not change much. This difference will disappear with an incremental increase of N_0 value.

7 Optimized structure and vibrational frequencies

The cutoff method selected makes a slight difference in determining the optimized geometry for the polymers. Tables 12 and 13 show the optimized geometries of *trans*-polyacetylene with the STO-3G and (7*s*3*p*/4*s*) basis sets, respectively. Optimization is performed by the energy gradient method, detail of which are already

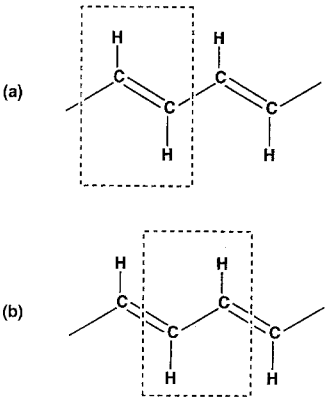

Fig. 3a, b. The two kinds of unit-cell structures of *trans*-polyacetylene: **a** Type 1 contains a C=C double bond, **b** Type 2 contains a C–C single bond

Table 11. Total energy of all-*trans*-polyacetylene using the Namur, cell-wise, modified symmetric, and symmetric cutoff methods. Types 1 and 2 represent the type of unit-cell. Energy is shown in a.u.

N_0	Namur		Cell-wise		Modified symmetric		Symmetric
	Type 1	Type 2	Type 1	Type 2	Type 1	Type 2	Type 1 and 2
2	−75.947852	−75.947440	−75.951134	−75.955765	−75.957108	−75.957461	−75.907321
3	−75.947907	−75.947842	−75.949545	−75.951909	−75.956408	−75.953093	−75.916140
4	−75.947919	−75.947907	−75.948899	−75.950319	−75.954201	−75.951270	−75.922185
5	−75.947291	−75.947919	−75.948573	−75.949515	−75.952885	−75.950323	−75.926393
10	−75.947922	−75.947923	−75.948099	−75.948351	−75.948099	−75.948824	−75.936199
20	−75.947923	−75.947923	−75.947969	−75.948034	−75.947969	−75.948295	−75.941819

published elsewhere [7, 8], using the threshold value of 10^{-4} Hartree/Bohr for residual force.

The Namur and cell-wise geometries almost converge at $N_0 = 2$ in both basis sets. The modified symmetric geometry is incorrect at $N_0 = 2$ because the C–C bond is too long and C=C bond is too short. These values, however, become almost correct at the STO-3G level with $N_0 \geqslant 3$ and at the (7*s*3*p*/4*s*) level with $N_0 \geqslant 4$. On the other hand, the symmetric cutoff results show poor convergence in both geometries and energies. We cannot obtain reasonable geometries for $N_0 = 2$ and 3 with the (7*s*3*p*/4*s*) basis set. Even after summation at $N_0 = 5$, the geometries are incorrect.

Table 14 shows the vibrational frequencies of the polyacetylene chain at the STO-3G level. The second derivative is calculated by two-point numerical differentiation of the first derivatives. The situation is the same for the vibrational frequency, as for the optimized geometries: The Namur, cell-wise, and modified symmetric cutoff schemes show reasonable agreement at a small N_0. The symmetric cutoff results show relatively slow convergence with respect to the N_0 value, reflecting the unsuitable bond lengths mentioned above, i.e., errors in the C–H stretching frequencies are too large. Both the optimized geometry and the vibrational frequency are less sensitive to the cutoff scheme than the total energy is [35].

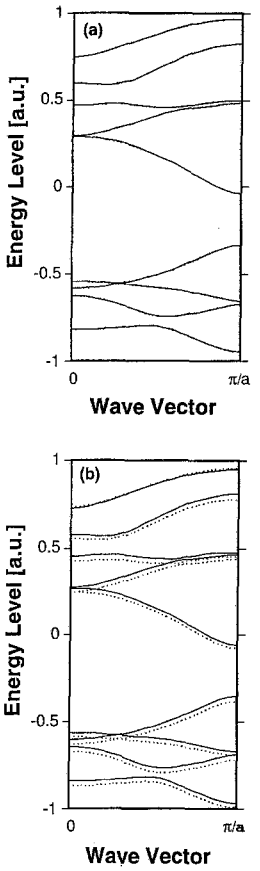

Fig. 4a, b. The (7*s*3*p*/4*s*) energy band structures of *trans*-polyacetylene. The straight line corresponds to a Type 1 unit cell and the broken line corresponds to a Type 2 unit cell. **a** Namur cutoff and **b** cell-wise cutoff

8 Comparison of CPU time

The comparison of the different cutoff methods based on the N_0 is reasonable. However, as easily shown from Eqs. (17) and (18), the Namur cutoff requires the large number of additional computation of the two electron integrals relative to the cell-wise cutoff and it is worthwhile to make a comment from the view of the computational efforts.

In Table 15 compares the CPU time on the IBM RS6000/59H workstation required to calculate the polyethylene chain with 4-31G basis set which is corresponding to the 4-31G part of Table 6.

As is easily seen from this table, the Namur $N_0 = 9$ is found to be comparable to cell-wise $N_0 = 15$ rather than $N_0 = 9$. In this sense, the Namur cutoff is not always superior to the cell-wise cutoff. We would also like to comment about the results of $N_0 = 7$ and 8. In these cases, we can obtain the SCF solution, but after considerable extra iterations comparing with $N_0 > 8$ case. Apparently, this is due to the insufficient summation of the exchange contribution to the total energy as the both cutoff methods give the same results. The selection of the cutoff scheme does not improve

Table 12. STO-3G optimized geometry and total energy of all-*trans*-polyacetylene with respect to the number of neighboring cells. Geometry units are shown in angstroems and degrees. Energy units are shown in a.u.

N_0	2	3	4	5
(a) Namur cutoff				
$R_{C=C}$	1.325	1.326	1.326	1.326
R_{C-C}	1.478	1.477	1.477	1.477
R_{C-H}	1.084	1.084	1.084	1.084
$\angle_{CCC}$	124.0	124.0	124.0	124.0
$\angle_{C=CH}$	119.8	119.8	119.8	119.8
Total energy	−75.947868	−75.947922	−75.947933	−75.947935
(b) Cell-wise cutoff				
$R_{C=C}$	1.327	1.326	1.326	1.326
R_{C-C}	1.475	1.476	1.476	1.477
R_{C-H}	1.084	1.084	1.084	1.084
$\angle_{CCC}$	124.2	124.1	124.0	124.1
$\angle_{C=CH}$	119.5	119.6	119.7	119.7
Total energy	−75.951136	−75.949551	−75.948904	−75.948581
(c) Modified symmetric cutoff				
$R_{C=C}$	1.315	1.326	1.326	1.326
R_{C-C}	1.489	1.473	1.474	1.475
R_{C-H}	1.085	1.083	1.083	1.084
$\angle_{CCC}$	124.1	124.0	123.9	123.9
$\angle_{C=CH}$	121.2	120.1	120.1	120.0
Total energy	−75.967567	−75.966457	−75.954246	−75.952922
(d) Symmetric cutoff				
$R_{C=C}$	1.318	1.322	1.324	1.324
R_{C-C}	1.503	1.495	1.491	1.488
R_{C-H}	1.106	1.098	1.096	1.093
$\angle_{CCC}$	126.9	125.8	125.3	125.0
$\angle_{C=CH}$	118.7	119.3	119.5	119.6
Total energy	−75.909496	−75.917023	−75.922676	−75.926695

the convergency and the choice of the Namur-type cutoff results in a waste of the computational time in such a case.

9 Concluding remarks

In this article, we have studied the results of *ab initio* crystal orbital calculations for various cutoff scheme. No long-range correction was performed. We have thoroughly studied the Namur cutoff and cell-wise cutoff schemes through calculations of polyethylene and LiH chains. The basis-set dependence of the total energy convergence with respect to the number of neighboring cells (N_0) and some

Table 13. (7*s*3*p*/4*s*) optimized geometry and total energy of all-*trans*-polyacetylene with respect to the number of neighboring cells. Geometry units are shown in angstroems and degrees. Energy units are shown in a.u.

N_0	2	3	4	5
(a) Namur cutoff				
$R_{C=C}$	1.388	1.388	1.388	1.388
R_{C-C}	1.530	1.529	1.529	1.529
R_{C-H}	1.185	1.185	1.185	1.185
$\angle_{CCC}$	122.6	122.6	122.6	122.6
$\angle_{C=CH}$	120.1	120.1	120.1	120.1
Total energy	−76.610083	−76.610090	−76.610094	−76.610095
(b) Cell-wise cutoff				
$R_{C=C}$	1.390	1.389	1.389	1.389
R_{C-C}	1.531	1.530	1.529	1.529
R_{C-H}	1.186	1.185	1.185	1.185
$\angle_{CCC}$	123.0	122.8	122.7	122.7
$\angle_{C=CH}$	119.5	119.7	119.8	119.9
Total energy	−76.611183	−76.610682	−76.610462	−76.610342
(c) Modified symmetric cutoff				
$R_{C=C}$	1.381	1.384	1.389	1.389
R_{C-C}	1.535	1.534	1.528	1.528
R_{C-H}	1.186	1.185	1.185	1.185
$\angle_{CCC}$	122.7	122.7	122.5	122.6
$\angle_{C=CH}$	123.0	121.9	120.6	120.5
Total energy	−76.617874	−76.614639	−76.612792	−76.612234
(d) Symmetric cutoff				
$R_{C=C}$	—	—	1.390	1.390
R_{C-C}	—	—	1.551	1.547
R_{C-H}	—	—	1.203	1.199
$\angle_{CCC}$	—	—	124.8	124.3
$\angle_{C=CH}$	—	—	119.0	119.3
Total energy	—	—	−76.575846	−76.581670

phenomena related to differences in the cutoff schemes were studied. These include the symmetry breaking problem, the dependence on the unit-cell structures of the calculated results, the optimized structure, and the vibrational frequency. The results of these studies have led to the following conclusions.

The Namur cutoff scheme gives the fastest energy convergence with respect to N_0, even without long-range corrections to the total energy. By applying the STO-3G , MINI, and (7*s*4*p*/3*s*) basis sets, we have found that the energy convergence behavior with respect to N_0 depends on the correlation between the basis set and cutoff scheme. The Namur cutoff shows the fastest convergence with the STO-3G basis set, intermediate convergence with the MINI basis set, and the slowest convergence with the (7*s*4*p*/3*s*) basis set. Cell-wise cutoff shows exactly

Table 14. Vibrational frequency of *trans*-polyacetylene at the STO-3G level ($k = 0$). Frequency units are shown in cm^{-1}

Cutoff	N_0	Vibrational frequencies[a]							
Namur	2	1086	1255	1335	1381	1548	2013	3684	3727
	3	1087	1255	1353	1381	1548	2009	3694	3715
	4	1087	1255	1352	1381	1548	2006	3695	3715
	5	1086	1255	1352	1380	1547	2006	3695	3715
Cell-wise	2	1093	1258	1360	1394	1549	2002	3681	3725
	3	1090	1257	1356	1388	1548	2000	3693	3713
	4	1089	1256	1354	1385	1548	2001	3693	3714
	5	1088	1256	1354	1383	1548	2003	3694	3714
Modified	2	1128	1272	1352	1393	1561	2063	3691	3708
Symmetric	3	1090	1262	1360	1395	1558	2005	3712	3731
	4	1091	1263	1359	1395	1558	2006	3710	3729
	5	1090	1261	1357	1392	1556	2006	3707	3727
Symmetric	2	1099	1240	1322	1369	1521	2041	3460	3500
	3	1085	1239	1327	1364	1525	2016	3544	3560
	4	1082	1241	1331	1365	1528	2007	3581	3597
	5	1081	1243	1334	1367	1531	2004	3603	3620

[a] Symmetries and mode assignments from left to right are: B_g C–H deformation out-of-plane. A_u C–H deformation out-of-plane, A_g C–C stretching, B_u C–H deformation in-plane, A_g C–C stretching with C–H deformation, A_g C–C stretching, A_g C–H stretching, and B_u C–H stretching

Table 15. Total CPU time in seconds on IBM RS6000/59H workstation. Numbers in parenthesis are the number of SCF cycles required

N_0	Namur	Cell-wise
7	997.770 (27)	656.740 (29)
8	834.390 (20)	557.500 (21)
9	658.740 (14)	428.130 (14)
10	742.460 (14)	415.950 (12)
15	902.060 (12)	663.110 (12)
20	1188.870 (12)	931.100 (12)
50	3132.250 (12)	2756.630 (12)
100	7585.720 (12)	6989.780 (12)

the reverse order. Even at the (7*s*4*p*/3*s*) level, the convergence is a little bit faster and smoother with the Namur cutoff than with cell-wise cutoff.

The Namur cutoff destroys the translational symmetry. This effect appears as asymmetry in the crystal orbital coefficients. Both the Namur and cell-wise cutoff introduce slight asymmetry on the two equivalent C–C bonds of polyethylene when calculating with a C_2H_4 unit cell. The asymmetry with the Namur cutoff disappears with increasing N_0, however, that with the cell-wise cutoff does not disappear within $N_0 \leqslant 10$.

Calculations for the two different unit-cell structures of *trans*-polyacetylene show the effects of the cutoff scheme on the total energy. Only the symmetric cutoff results are the same. The disagreement for the Namur cutoff disappears at $N_0 = 20$; however, that for the cell-wise and modified symmetric cutoff does not disappear within $N_0 \leqslant 20$. Thus, it is necessary to choose the unit cell carefully when comparing the energy values among the isomers.

The optimized geometry and vibrational frequency are not as sensitive to the cutoff method as the total energy itself, except with the symmetric cutoff. The Namur and the cell-wise cutoff schemes give almost the same values. The modified symmetric cutoff scheme shows a slightly slower convergence with respect to N_0. All three schemes show reasonable agreement at $N_0 = 5$. The symmetric cutoff, however, does not give reasonable geometry nor reasonable vibrational frequencies.

All these results combined show that the Namur cutoff is the superior cutoff scheme, when calculating the insulator using the relatively compact minimal basis sets, especially the STO-3G basis set. Although it introduces slight asymmetry in the matrix elements, attempts to remove this asymmetry result in the slower convergence of the total energy with respect to the number of neighboring cells. It is found, however, to be a waste of time to employ the Namur cutoff when calculating with the more extended 4-31G basis sets.

The next step of this work is to incorporate electron correlation into the calculations.

Acknowledgements. The author is grateful to Dr. Jim Maxka for his stimulating discussions and suggestions. Thanks are also due to Dr. Sandor Suhai of German Cancer Center for providing the original crystal orbital program.

References

1. Kertész M, Koller J, Azman A (1977) J Chem Phys 67: 1180
2. Kertész M, Koller J, Azman A (1978) Chem Commun 575
3. Kertész M, Koller J, Azman A (1979) Phys Rev B 19: 2034
4. Karpfen A, Höller R (1981) Solid State Commun 37: 179
5. Suhai S (1980) J Chem Phys 73: 3843
6. Dovesi R (1984) Int J Quantum Chem 26: 197
7. Teramae H, Yamabe T, Imamura A (1984) J Chem Phys 81: 3564
8. Teramae H, Satoko C, Yamabe T, Imamura A (1983) Chem Phys Lett 101: 149
9. Teramae H (1986) J Chem Phys 85: 990
10. Delhalle J, Piela L, Brédas JL, André JM (1980) Phys Rev B 22: 6254
11. André JM, Vercauteren DP, Bodart VP, Fripiat JG (1984) J Comput Chem 5: 535
12. Suhai S (1992) Int J Quantum Chem 42: 193
13. Karpfen A, Beyer A (1984) J Comput Chem 5: 11
14. Del Re G, Ladik J, Biczo G (1967) Phys Rev 155: 997
15. André JM (1969) J Chem Phys 50: 1536
16. (a) Ukrainskii II (1975) Theoret Chim Acta 38: 179; (b) Monkhorst HJ, Kertész M (1981) Phys Rev B 24: 3015; (c) Piela L, André JM, Fripiat JG, Delhalle J (1981) Chem Phys Lett 77: 143; (d) Delhalle J, Calais JC (1986) Phys Rev B 34: 5826
17. André JM, Leroy G (1971) Int J Quantum Chem 26: 557
18. Yamabe T et al. (1979) J Phys C: Solid State Phys 12: L257
19. Yamabe T et al. (1979) Solid State Commun 29: 329
20. Karpfen A (1981) Int J Quantum Chem 19: 1207
21. Imamura A (1970) J Chem Phys 52: 3186

22. Fujita H, Imamura A (1970) J Chem Phys 53: 4555
23. Morokuma K (1970) Chem Phys Lett 6: 186
24. Morokuma K (1971) J Chem Phys 54: 962
25. Blumen A, Merkel C (1977) Phys Status Solidi B 83: 425
26. Teramae H, Takeda K (1989) J Am Chem Soc 111: 1281
27. Otto P, Clementi E, Ladik J (1983) J Chem Phys 78: 4547
28. Davis PJ, Rabinowitz P Method of numerical integration. Academic Press, New York, 1975, p 45
29. Karpfen A (1981) J Chem Phys 75: 238
30. Gianolo L, Pavani R, Clementi E (1978) Gazz Chim Ital 108: 181
31. Hehre WJ, Ditchfield R, Stewart RF, Pople JA (1970) J Chem Phys 52: 2769
32. Although André et al. [11] reported their geometry as $r_{CC} = 1.09$ a.u. and $r_{CH} = 1.54$ a.u., we suppose these are the miss prints of $r_{CC} = 1.54$ Å and $r_{CH} = 1.09$ Å.
33. Surján PR, Kertész M, Karpfen A, Koller J (1983) Phys Rev B 27: 7583
34. Kertesz M (1982) Adv Quantum Chem 15: 161
35. Cionslowski J (1988) Chem Phys Lett 153: 446; Cui CX, Kertesz M, Jiang Y (1990) J Phys Chem 94: 5172